

# Pyroelectric and piezoelectric properties of thick PZT films produced by a new sol–gel route

M. Es-Souni\*, M. Kuhnke, A. Piorra, C.-H. Solterbeck

*University of Applied Sciences, Institute for Material and Surface Technology (IMST), Kiel, Germany*

Available online 25 March 2005

## Abstract

The pyroelectric and piezoelectric properties of thick PZT films processed via a new sol–gel method are being investigated. The films were deposited on gold-coated alumina substrates. The pyroelectric properties are being evaluated using pyrodynamic measurements with either a laser or thermoelectric heat source. The pyroelectric coefficient is obtained from pyroelectric current measurements. The piezoelectric properties are being measured using a laser vibrometer-lock-in amplifier set-up. It is shown that the pyroelectric coefficient obtained with laser heating lies in the range of  $108 \mu\text{C}/\text{m}^2 \text{K}$ , whereas heating from the rear of the specimen with the thermoelectric element lead to a value of in the range of  $350 \mu\text{C}/\text{m}^2 \text{K}$ . These results are explained in terms through thickness temperature gradients. The piezoelectric displacement amplitude versus applied voltage shows a no-linear behaviour, which is explained in terms of materials chemistry. The maximum effective piezoelectric coefficient,  $d_{33}$ , is obtained as  $340 \text{ pm}/\text{V}$ , and is superior to the values known for ferroelectric thin films.

© 2005 Elsevier Ltd. All rights reserved.

*Keywords:* Sol–gel processes; Microstructure-final; Piezoelectric properties; PZT; Functional applications

## 1. Introduction

The use of ferroelectric materials in low-cost infrared detection and thermal imaging systems as well in high power piezoelectric applications, e.g. sensors and actuators, is well established.<sup>1–3</sup> The materials of choice for such applications are based on the  $\text{PbTiO}_3$ – $\text{PbZrO}_3$  (PZT) solid solution system in bulk ceramic form. In the last years, however, ferroelectric thin films are being intensively investigated for micro-actuators, micro-electromechanical-systems<sup>4</sup> (MEMS) and thin film IR-sensor arrays.<sup>3</sup> The films can be processed cost-effectively at temperatures far below those required for bulk ferroelectrics. Furthermore, compatibility with silicon technology presents the advantage of active film deposition directly on read-out circuitry which can result in cheap devices.<sup>5</sup> A versatile method for the processing of thin films is via solution deposition which allows films of up to  $1 \mu\text{m}$  thickness to be fabricated in a cost-effective way. Thicker films can be achieved by spin-coating a sol filled with fine

dispersion of ceramic particles.<sup>6,7</sup> In recent work<sup>7</sup> we showed that it is possible to process thick, crack-free and dense PZT films using this processing route. The purpose of this work is to investigate the pyroelectric and piezoelectric properties of these films deposited on gold-coated alumina substrates.

## 2. Experimental details

Ferroelectric films of  $5 \mu\text{m}$  thickness were prepared using a propriety method.<sup>7</sup> Milled powders of PZT (PZ21 Ferroperm, DK) were mixed with a PZT52/48 sol and spin-coated on gold-coated alumina (alumina 99.6%, CeramTech, Germany) substrates. The gold coating was also performed using spin-on technique. After pyrolysis and sintering for 30 min at  $800^\circ\text{C}$ , the films were infiltrated with the PZT52/48 sol and annealed at  $700^\circ\text{C}$  for 30 min to give a dense film. The microstructure of the film, including surface topography and cross section, was investigated by means of scanning electron microscopy (SEM). Pt top electrodes were sputtered onto the film surface to provide the electrical front contacts. For piezoelectric and pyroelectric measurements, the front elec-

\* Corresponding author. Tel.: +49 431 210 2660; fax: +49 431 210 2661.  
E-mail address: [mohammed.es-souni@fh-kiel.de](mailto:mohammed.es-souni@fh-kiel.de) (M. Es-Souni).

trodes with an area of 6.69 mm<sup>2</sup> consisted of a central circular pattern with four adjacent contact pads. The samples were measured in the corona poled states (15 kV was applied for 20 min at 150 °C, and the specimens were cooled down under bias).

The impedance measurements were performed in the frequency range from 100 Hz to 1 MHz with a computer controlled impedance analyser. The Curie temperature  $T_C$  of the film was measured on cooling at a frequency of 1 kHz.

Pyrodynamic and bolometric measurements were made using a self-made experimental set-up. The thermal excitation is done sinusoidally with a thermoelectric heater/cooler element (Peltier element) or a near-infrared laser ( $\lambda = 681.8$  nm, output power amplitude: 9.6 mW). Mean temperature of all measurements was room temperature.

Surface temperature measurements were performed using the front electrode as a bolometer. The lock-in amplifier was employed to monitor the bolometric voltage variation. The Pt electrode is contacted with two needles and the current and voltage is supplied and measured separately at the two needles (4-wire sense). An evaluation method using the two first order Fourier coefficients of the temperature and voltage signals is applied to determine the amplitudes. From the amplitudes the calibration coefficient is calculated. The bolometric calibration was done twice and the coefficients values of 0.6131 and 0.6162 °C/mV obtained were close to each other. The dependence of surface temperature on the modulation frequency of thermal excitation is computed from the measured bolometric voltage amplitude and the above-mentioned coefficient. For the Peltier element the frequency was in the range from 30 to 200 mHz and for the laser in the range from 100 mHz to 1 kHz.

The piezoelectric measurements were done using a self-made experimental set-up including a computer controlled laser interferometer (Polytec OFV 353 sensor head and OFV 3001 vibrometer controller), DSP lock-in amplifier, frequency generator and voltage source. The vibrometer was operated in the most sensitive velocity range (1 mm/s/V). The position of the laser spot was in the centre of investigated front electrode.

### 3. Results and discussion

#### 3.1. Microstructure

The surface topography of the PZT films (not shown) shows a crack-free bimodal structure consisting of fine grains and rosette-like coarse grains.<sup>7</sup> The XRD-patterns (not shown) reveal phase pure perovskite without pyrochlore. The cross-section microstructure of the film shown in Fig. 1 reveals quite compact films. It should be pointed out that the processing method outlined above leads to reproducible film microstructures both on platinumized silicon, reported in a previous work,<sup>7</sup> and gold-coated alumina.

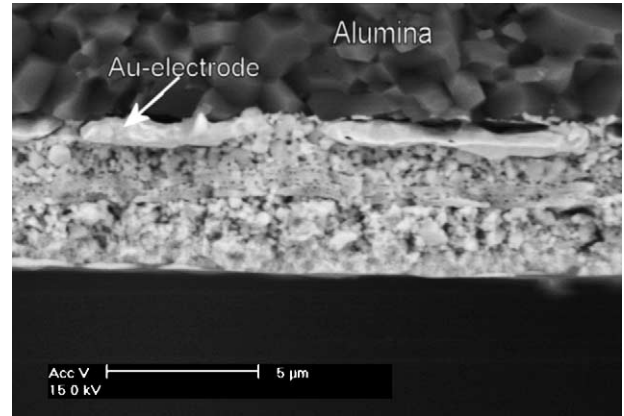


Fig. 1. Back-scattered electron micrographs of PZT film cross-section.

#### 3.2. Pyroelectric properties

The pyroelectric coefficient is obtained from measuring the resulting pyroelectric current or charge as a consequence of temperature changes in the ferroelectric material.<sup>1</sup> For sinusoidal temperature modulation the pyroelectric coefficient of a ferroelectric film can be calculated from the pyroelectric current:

$$p_i(\omega) = \frac{\Delta i_p(\omega)}{\omega \Delta T(\omega) A} \quad (1)$$

where  $p_i(\omega)$  is the pyroelectric coefficient,  $\Delta i_p(\omega)$  the amplitude of the pyroelectric current,  $\Delta T(\omega)$  the amplitude of the temperature modulation and  $A$  the area of the front contact. It is assumed that the temperature variation is homogenous in the ferroelectric film and hence equal to the surface temperature of the film.

In Fig. 2 the magnitudes of the effective bolometer voltage and surface temperature using the sinusoidally modulated laser and the Peltier element as heat sources are shown. Multiplying the magnitude by  $\sqrt{2}$  and 0.6162 °C/mV (calibration factor, see above) gives the peak amplitude of the surface temperature. As expected, the surface temperature decreases with increasing frequency. At  $f > 3$  Hz an enhanced decrease of the

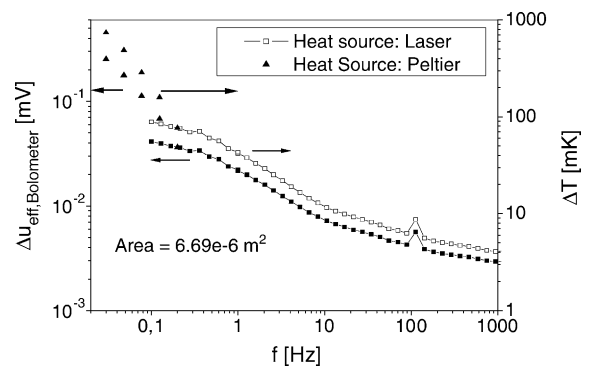


Fig. 2. Effective bolometer voltage and surface temperature amplitudes using the sinusoidally modulated laser and Peltier element as heat sources.

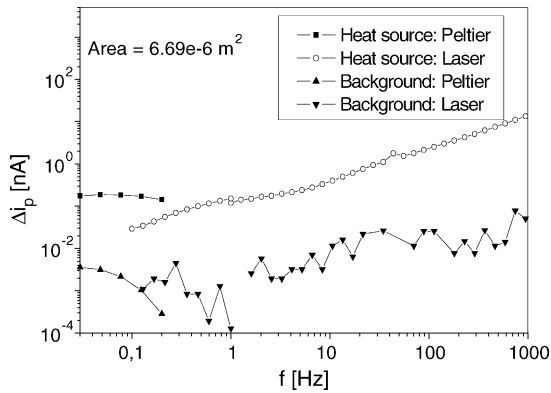


Fig. 3. The pyroelectric current using Peltier element and laser as heat sources together with the background measurements are shown.

voltage signal of the bolometer appears. However, the intensity of the sinusoidally modulated laser light is nearly constant in the whole frequency range. One suggestion is that for high frequencies the lateral surface temperature distribution becomes inhomogeneous, since the thermal diffusion length  $\sqrt{D/f}$  ( $D = \lambda/c\rho$ ,  $\lambda$  is the thermal conductivity,  $c$  the thermal capacity and  $\rho$  the density of platinum. The values can be found in standard hand books.) of approximately 2.8 mm at 3 Hz is less than the dimension of the bolometer, and resembles more the intensity profile of the laser spot. Therefore, the contribution of the adjacent pad areas diminishes, and the measured voltage signal corresponding to temperature variation integrated over the whole bolometer area decreases. Numerical simulations have to prove the validity of this suggestion. Using the Peltier element as a heat source the surface temperature increases with decreasing frequency because of the slow response of the Peltier element.

Fig. 3 illustrates the pyroelectric currents obtained using either the laser or the Peltier element as heat sources. Using the laser as the heat source, the pyroelectric coefficient  $p_i$  obtained from Eq. (1) is almost frequency independent in the frequency range  $f = 0.1$ –1000 Hz, and the mean value calculated is  $p_i = 108.5 \mu\text{C/K m}^2$ . The mean value of the pyroelectric coefficient calculated from the pyroelectric current using the Peltier element as the heat source amounts to  $p_i = 352 \mu\text{C/K m}^2$ , and is frequency independent. This pyroelectric coefficient is suggested to be closest to the real value, since the specimen is homogeneously heated from the rear side and no temperature gradient occurs. The pyroelectric coefficient  $p_i$  using the laser as heat source is 3.2 times

smaller than the aforementioned pyroelectric coefficient. One assumes that a temperature gradient from the sample surface into the ferroelectric film causes the difference. Nevertheless, while the pyroelectric coefficient obtained using the Peltier element probably reflects a material property, the one obtained using the laser as heat source is supposed to better reflect device performance.

The figures-of-merit of response  $F_V$  and detectivity  $F_D$  for a detector element are listed in Table 1 using a volume specific heat capacity  $c' = 2.5 \text{ J/cm}^3/\text{K}$ .<sup>1</sup> The figures-of-merit agree reasonably with the values obtained from literature for sol–gel films (data compiled in reference).<sup>5</sup> Only the high loss tangent and the high dielectric constant of the ferroelectric films obviously degrades  $F_D$ , and devices built with this material are supposed to have a higher dielectric-loss generated Johnson noise than one reported for modified PZT ceramics,<sup>1</sup> Table 1.

### 3.3. Piezoelectric properties

For the simple case, when a sinusoidally modulated voltage is applied to a piezoelectric material, the displacement amplitude,  $\Delta L_n$ , can be calculated from surface velocity amplitude

$$\Delta L_n = \frac{\Delta v_n}{n\omega} \quad (2)$$

where  $\Delta v_n$  is the surface velocity amplitude,  $\omega$  the angular frequency and  $n$  an integer designating the order of the harmonic. The piezoelectric coefficient is given by

$$d_{xy}^{(n)} = \frac{\Delta L_n}{\Delta V^n} \quad (3)$$

where  $\Delta V$  is the amplitude of the sinusoidal modulated voltage. The indices  $x$  and  $y$  depend on the direction of the applied electric field and the direction of induced displacement regarding symmetry-axis of the piezoelectric crystal.<sup>1</sup>

Fig. 4a shows the piezoelectric displacement amplitude versus the applied voltage amplitude both for the first harmonic (piezoelectric effect) and the second harmonic (electrostrictive effect). It can be seen that the piezoelectric displacement  $\Delta L_1$  is not a linear function of  $\Delta V$ . The curve can be fitted to two straight lines with  $d_{33}$  of the order of 160 pm/V at low voltages and 340 pm/V at high voltages. The results suggest that the piezoelectric displacement arises from the superposition of the contributions from the sol and

Table 1

The dielectric, pyroelectric and piezoelectric properties of the investigated PZT film and a standard PZT ceramic from literature are listed

Material	$T$ (°C)	$\epsilon'$	$\tan \delta$	$p$ ( $\mu\text{C/K m}^2$ )	$T_C$ (°C)	$c'$ ( $\text{J/m}^3/\text{K}$ )	$F_V$ ( $\text{m}^2/\text{C}$ )	$F_D$ ( $\text{Pa}^{-1/2}$ )	$d_{33}$ (pm/V)
PZT film	21–23	558	0.022	352	220	$2.5 \times 10^6$	$2.8 \times 10^{-2}$	$1.4 \times 10^{-5}$	340
PZT ceramic	–	290	0.0027	380 <sup>a</sup>	230	$2.5 \times 10^6$	$6.0 \times 10^{-2}$	$5.8 \times 10^{-5}$	685 <sup>b</sup>
PZT thick film <sup>6</sup>	–	900	–	–	420	–	–	–	325

<sup>a</sup> Modified PZT ceramics (PZFNUTU).

<sup>b</sup> Sintered PZ21 ceramics (materials data sheet, Ferroperm).

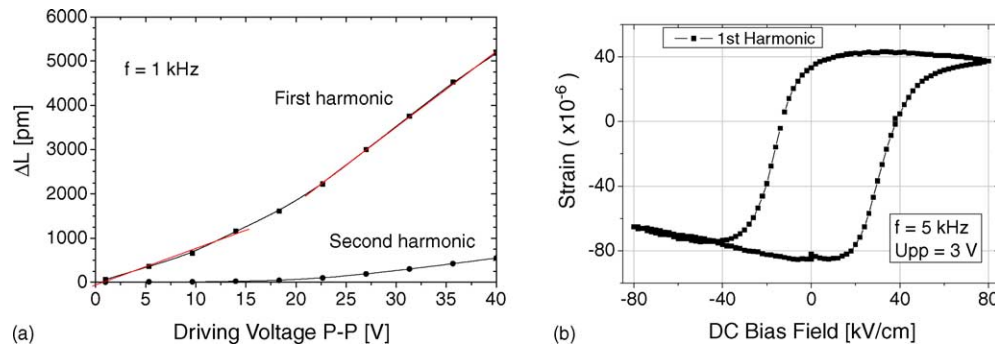


Fig. 4. (a) Piezoelectric (first harmonic) and electrostrictive (second harmonic) displacement amplitudes vs. applied voltage and (b) piezoelectric hysteresis curve showing strain as a function of applied dc bias field for the PZT film investigated.

the powder, which constitute two phases with different stoichiometries and therefore different piezoelectric properties. The values of  $d_{33}$  are lower than those of sintered PZ21 ceramics reported in the materials data sheet (Ferropem Piezoceramics A/S) but are superior to those reported for PZT thin films.<sup>8</sup> Barrow et al.<sup>6</sup> report a  $d_{33}$  value of 325 pm/V on a 20  $\mu\text{m}$  PZT thick film, which is close to that of the present work. The piezoelectric hysteresis loop can be seen in Fig. 4b. An almost square hysteresis loop is obtained with a high remnant strain. This behaviour is usual for soft, i.e. donor doped, PZT ceramics. However, it can also be seen that the hysteresis loop is asymmetric both in the strain and field axis which is indicative of an internal bias field.

Although the present results can be first considered as preliminary, and need complementary investigations, e.g. determination of the in-plane piezoelectric coefficient  $d_{31}$ , they nevertheless show the promising potentials of these films in micro-actuator applications.

#### 4. Summary and conclusion

For the determination of the pyroelectric coefficient of a ferroelectric film from pyrodynamic measurements the pyroelectric current is more suitable than the pyroelectric voltage, since the uncertainty in the film capacitance is avoided. Also a thermal excitation of the sample from the rear side, using a thermoelectric heater/cooler or Peltier element, which ensures a homogeneous heating of the ferroelectric film, is necessary. The 5  $\mu\text{m}$  thick PZT film prepared with the powder-sol method is a suitable ferroelectric material for infrared detection at room temperature. The dielectric and pyroelectric properties of the ferroelectric film given in Table 1 agree reasonably with the values from literature. The relatively large dielectric loss of this thick film ( $\tan \delta = 0.022$ ) in comparison with other PZT films may be due to relaxation phenomena both at the powder/sol interfaces, since they are of different stoichiometries, and at the film electrode interface. However, the pyroelectric coefficient  $p = 352 \mu\text{C/K/m}^2$  obtained is large for a PZT film. The high relative permittivity  $\epsilon' = 558$  of the investigated PZT

film suggest an application for small area detector elements, e.g. an array of detector elements for thermal imaging. The figure-of-merit of voltage response  $F_V = 2.8 \times 10^{-2} \text{ m}^2/\text{C}$  is similar to other PZT films but smaller than that of modified PZT ceramics. This also holds for the figure-of-merit of specific detectivity  $F_D = 14 \times 10^{-6} \text{ Pa}^{-1/2}$  which is by a factor 4 smaller compared to modified PZT ceramics, and hence the detector has a higher dielectric-loss generated Johnson noise.

The piezoelectric properties of the films are promising for micro-actuator applications. They can be further improved by choosing a sol stoichiometry closer to that of the PZT powder material.

In conclusion, the present work shows that it is possible to obtain good quality thick PZT films via spin-coating a colloidal sol-powder solution. This processing route allows such films to be obtained in few coating sequences. It offers a good control of film thickness and microstructure, and is in this respect superior to the screen-printing method. As can be inferred from pyroelectric and piezoelectric measurements, the films can be used both in pyroelectric and piezoelectric applications.

#### Acknowledgement

The financial support of the Federal Ministry of Education and Research (Grant Nr. 1700602) is gratefully acknowledged.

#### References

1. Moulson, A. J. and Herbert, J. M., *Electroceramics*. John Wiley & Sons, Chichester, 2003, 339–432.
2. Amin, A., The role of connectivity in thermal imaging. *J. Electroceram.*, 2002, **8**, 99–106.
3. Lang, S. B. and Das-Gupta, D. K., Pyroelectricity: fundamental and applications. In *Handbook of Advanced Electronic and Photonic Materials and Devices: Ferroelectrics and Dielectrics*, Vol. 4, ed. H. S. Nalwa. Academic Press, New York, 2001, pp. 1–55.
4. Polla, D. L. and Francis, L. F., Ferroelectric thin films in micro-electromechanical devices. *Mater. Res. Soc. Bull.*, 1996, **21**(7), 59–65.

5. Whatmore, R. W. and Watton, R., Pyroelectric materials and devices. In *Infrared Detectors and Emitters*, ed. P. Capper and C. T. Elliott. Kluwer Academic Publishers, Norwell, MA, 2001, pp. 120–124.
6. Barrow, D. A., Petroff, T. E., Tandon, R. P. and Sayer, M., Characterization of thick lead zirconate titanate thin films using a new sol–gel based process. *J. Appl. Phys.*, 1997, **81**, 876–881.
7. Es-Souni, M. and Piorra, A., Processing and characterization of high-quality thick PZT films. *Ferroelectrics*, 2003, **293**, 63–68.
8. Lian, L. and Sottos, N. R., Effects of thickness on the piezoelectric and dielectric properties of lead zirconate titanate thin films. *J. Appl. Phys.*, 2000, **87**, 3941–3949.